LAGλ-1: A clinically relevant drug resistant human multiple myeloma tumor murine model that enables rapid evaluation of treatments for multiple myeloma

RICHARD A. CAMPBELL[1], STEVEN J. MANYAK[1], HONGHAO H. YANG[2], NELIDA N. SJAK-SHIE[3], HAIMING CHEN[1], DORINA GUI[6], LAURA POPOVICIU[6], CATHY WANG[1], MELINDA GORDON[1], SHEN PANG[4], BENJAMIN BONAVIDA[5], JONATHAN SAID[6] and JAMES R. BERENSON[1]

[1]Institute for Myeloma & Bone Cancer Research, West Hollywood, CA 90069; [2]Pacific Shores Medical Group, Glendale, CA 91204; [3]The Center for Cancer Care & Research, St. Louis, MO 63141; [4]Department of Dentistry and Oral Biology, UCLA School of Dentistry and the Departments of [5]Microbiology, Immunology and Molecular Genetics and [6]Pathology and Laboratory Medicine, Geffen School of Medicine at the University of California at Los Angeles, Los Angeles, CA 90095, USA

Received January 23, 2006; Accepted February 24, 2006

Abstract. We set out to generate new human myeloma tumors that grow in immunodeficient mice and can be used for pathophysiological studies and rapid evaluation of new therapies. Fresh whole core bone marrow (BM) biopsies taken from 33 myeloma patients were engrafted into the hind limb muscle of severe combined immunodeficient (SCID) mice. Human Ig was detected in 28/33 mice and three grew palpable tumors displaying many features of human myeloma including morphology, immunophenotype and BM plasmacytosis. Following intramuscular passage, we generated large numbers of mice with predictable increases in tumor growth and human paraprotein levels. We further characterized the model generated from an IgGλ-producing tumor known as LAGλ-1 and determined the effects of the proteasome inhibitor bortezomib, the alkylating agent melphalan, and the DNA damaging agent liposomal doxorubicin, on the growth of this tumor. LAGλ-1-bearing mice receiving higher doses of bortezomib showed reduced tumor growth whereas a lower dose had no effect. In contrast, melphalan did not significantly alter tumor growth, except minimally at high doses, reflecting the resistance of this patient's tumor to this drug. We also used our intramuscular (i.m.) LAGλ-1 model to optimize the dosing schedule of liposomal doxorubicin. Low doses administered once daily three days per week decreased tumor growth and human paraprotein levels whereas much higher doses given once weekly had no anti-myeloma effects. Furthermore, LAGλ-1 cells produce local tumors when injected subcutaneously and lytic lesions when injected intravenously allowing for multiple methods of evaluating the anti-myeloma effects of a variety of agents. Our new clinically relevant SCID models of human myeloma should greatly facilitate drug development and enable novel therapies to quickly move from the laboratory to the clinic.

Correspondence to: Dr James R. Berenson, Institute for Myeloma & Bone Cancer Research, Suite 300, 9201 Sunset Blvd., West Hollywood, CA 90069, USA
E-mail: jberenson@myelomasource.org

Key words: multiple myeloma, murine model, SCID mouse, animal model

Introduction

Multiple myeloma (MM) is a malignancy characterized by the proliferation of monoclonal plasma B cells in the bone marrow (BM). It is the second most common hematologic malignancy in the US with an incidence of 15,000 new cases per year. This disease is associated with a serum monoclonal (M) protein or immunoglobulin, development of osteolytic lesions and bone resorption. Currently, there are numerous treatment modalities for MM but the disease remains incurable. With the recent addition of novel anti-myeloma therapies to the treatment arsenal, there exists a need for *in vivo* models of human MM that are both biologically and clinically relevant, and allow for rapid and efficient evaluation of drug therapies and new targets for treating this B-cell malignancy.

Human MM cell lines have commonly been used for developing *in vivo* models (1-7). The advantage of these models has been the ability to produce large numbers of experimental animals in short periods of time. Although these cell lines readily grow consistent tumors in SCID mice, the resulting models often have few similarities to human MM. In addition, these immortalized cell lines grow *in vitro*, independent of the human BM microenvironment, further demonstrating biological characteristics and growth patterns more similar to plasma cell leukemia or aggressive lymphomas rather than typical MM *in vivo*.

Several new animal models have been generated either through the injection of purified myeloma cells from MM patient bone marrow aspirates (8-14) or the implantation of

human fetal or rabbit bones into immunodeficient mice followed by injections of purified myeloma cells from MM patient bone marrow aspirates (15-17). These cells were successfully engrafted >50% of the time and eventually led to the appearance of serum paraprotein and, in some cases, extramedullary tumors. While these models are widely used to study the biology of myeloma and its manifestations, they are limited to the amount of cells obtained from each patient sample and cannot generate large cohorts of animals bearing tumor. In addition, the primary myeloma cells disappeared after complete resorption of the fetal bone implants, indicating that the myeloma cells could not grow without the human fetal bone microenvironment in the mice.

We describe in detail one novel MM model and its usefulness in evaluating a variety of anti-myeloma agents. One IgG-producing patient's tumor, known as LAGλ (Los Angeles IgG λ light chain)-1, was more fully characterized and underwent continuous passage in the murine muscle. SCID mice inoculated or engrafted with LAGλ-1 cells develop clinical manifestations of human myeloma including increased levels of serum monoclonal paraprotein, cell morphology, bone marrow plasmacytosis, and ultimately bone resorption. LAGλ-1 maintains the parent tumor characteristics. These myeloma implants can provide large cohorts of SCID mice growing tumors with consistent growth patterns in a very short period of time for rapid evaluation of preclinical studies. LAGλ-1 was derived from a patient resistant to melphalan treatment. We found that this chemoresistant phenotype was maintained as reflected by LAGλ-1's ability to grow *in vivo* even in the presence of high- dose melphalan.

This study examined the following: 1) the ability of LAGλ-1 to propagate in SCID mice via administration by various routes intramuscular, intravenous and subcutaneous (i.m., i.v., s.c.); 2) the stability of LAGλ-1's drug-resistant phenotype acquired from the patient; and 3) the *in vivo* response on i.m. administration of LAGλ-1 following treatment with various chemotherapeutic drugs.

Materials and methods

Patient samples. Fresh bone marrow biopsies from 33 patients diagnosed with MM were obtained following informed consent per Cedars-Sinai Medical Center and the Institutional Review Board (IRB) protocols. The Ig heavy and light chain isotypes were determined at diagnosis by immunofixation electrophoresis (IFE).

Animals. Six-to-eight-week-old homozygous C.B-17 *SCID/SCID* (severe combined immunodeficient, SCID) mice were obtained from Harlan Sprague Dawley (Indianapolis, IN) and were maintained in a pathogen-free area in our resources facility. All animal studies were conducted according to protocols approved by the Cedars-Sinai Institutional Animal Care and Use Committee (IACUC).

Cells and culture conditions. The RPMI-8226 MM cell line (American Type Culture Collection, Manassas, VA) was cultured in RPMI-1640 (Omega Scientific, Tarzana, CA) supplemented with 10% fetal bovine serum (FBS), 2 mM L-glutamine, 50 units/ml penicillin, and 50 μg/ml streptomycin (all Omega Scientific, Tarzana, CA). Prior to s.c. tumor cell injection into mice, cells were washed twice and re-suspended in RPMI-1640 with 10% FBS at a concentration of $5x10^6$ cells/100 μl.

Patient primary intramuscular bone marrow biopsy implants. Six-to-eight-week-old male SCID mice were irradiated with 250 cGy, and anesthetized with ketamine, xylazine, and isoflurane prior to surgery. Fresh myeloma patient bone marrow biopsies (2.0-4.0 mm^3) were implanted into the superficial gluteal muscle of the left hind limb. Starting on the day of surgery, mice received a weekly injection of anti-asialo GM1 rabbit sera (Wako Bioproducts, Richmond, VA) to further suppress NK-mediated immune activity. Tumor volume was measured weekly using calipers and the following formula: $4/3\pi$ x $(\text{width}/2)^2$ x (length/2), accurately portraying the three-dimensional volume of an ellipsoid (18). Human paraprotein levels were measured weekly (see below).

The LAGλ-1 mouse

Intramuscular model. A growing LAGλ-1 i.m. tumor was excised from a donor mouse, sectioned, and surgically implanted as described above. Tumor volume was measured as described above and tumor clonality was determined by IFE using standard clinical techniques.

Subcutaneous model. A growing fourth generation LAGλ-1 i.m. tumor was excised from a donor mouse, sectioned and digested using pronase-E (EMD Chemicals, Gibbstown, NJ). The cells were filtered over autoclaved 200 μm nylon mesh filters (BioDesign Inc, New York, NY) in order to produce a single cell suspension. The cells were washed 3 times in PBS, counted and assessed for viability using trypan blue exclusion. SCID mice irradiated as before received s.c. injections of $3x10^6$ LAGλ-1 cells suspended in 200 μl RPMI-1640 or 100 μl RPMI-1640 with or without 100 μl of Matrigel basement membrane matrix (Becton Dickinson, Bedford, MA) into the right flank. Tumor volume was measured weekly using calipers and human IgG (hIgG) serum levels were measured weekly by ELISA, as described below.

Intravenous model. A fifth generation LAGλ-1 i.m. tumor was excised from the mouse and single cell suspensions were prepared as described above. Irradiated SCID mice received an i.v. injection of $5x10^6$ LAGλ-1 cells into the tail vein.

Determination of human IgG (hIgG) levels. Levels of human IgG subclass 1 were determined by enzyme-linked immunosorbent assay (ELISA). Human IgA, IgM, IgG, and IgG subclass profile ELISA kits were purchased from Zymed Laboratories (South San Francisco, CA). Mice bearing LAGλ-1 tumors were bled weekly via retro-orbital bleed. Samples were spun at 13,000 rpm for 30 min and serum collected. The IgG subclass 1 ELISA kit was prepared according to the manufacturer's specifications. Absorbance at 450 nm with a reference wavelength of 550 nm was determined on a μQuant microplate spectrophotometer with KC Junior software (Bio-Tek Instruments, Winooski, VT).

Histopathology. At the time of sacrifice, tumors and organs were excised from the animals, fixed in 10% neutral-buffered formalin and embedded in paraffin according to standard

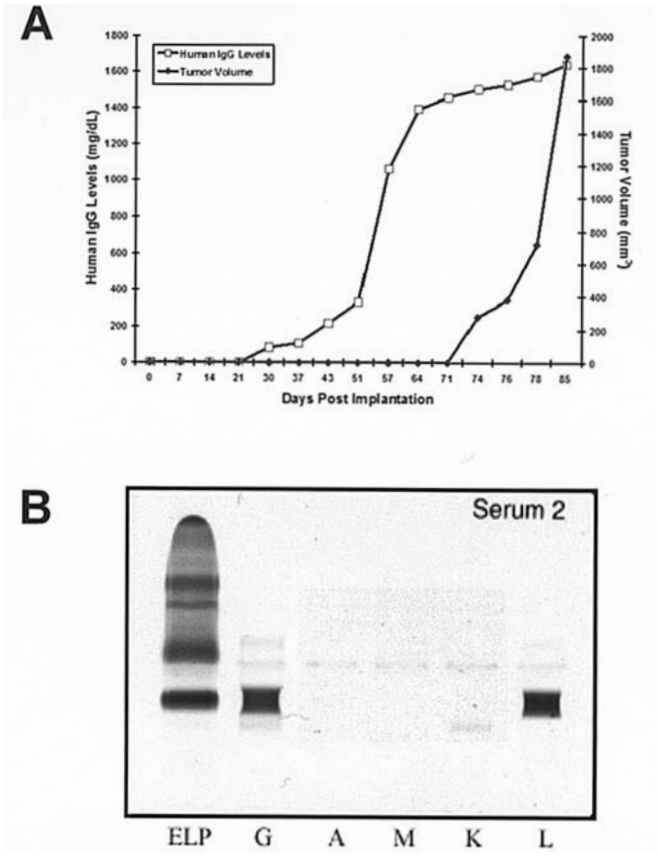

Figure 1. Tumor growth and serum hIgG secretion in a SCID mouse following i.m. implantation of an MM patient bone marrow biopsy. (A) Tumors were measured weekly using standard calipers and hIgG was measured weekly by ELISA. (B) IFE identifies the paraproteins present in the mouse serum as hIgG heavy chain and hIgλ light chain as shown by the distinct bands.

histological procedures. Sections measuring 4-5 μm were deparaffinized in xylene, rehydrated with ethanol, and rinsed in PBS. The deparaffinized sections were stained with hematoxylin and eosin (H&E) for morphological analysis. Cells were analyzed by immunofluorescent assay (IFA) using polyclonal goat anti-hIgG FITC (CALTAG Laboratories, Burlingame, CA) and mouse monoclonal anti-CD38 PE (clone HIT2, BD Biosciences, Franklin Lakes, NJ). Immunohistochemical (IHC) staining was performed on deparaffinized sections with anti-cytomegalovirus (CMV, clone CCH2), and anti-Epstein-Barr virus latent membrane protein (EBV LMP, clone CS.1-4, both Dako, Carpinteria, CA) streptavidin-conjugated antibodies using an avidin-biotin complex detection system (Vector Laboratories, Burlingame, CA) according to the manufacturer's instructions.

Flow cytometry. A single cell suspension of LAGλ-1 was prepared as described above. One million LAGλ-1 cells were singly stained on the surface with anti-CD19 FITC (clone SJ25-C1, CALTAG Laboratories), anti-CD20 FITC (clone 2H7), anti-CD38 PE (clone H1T2), anti-CD45 FITC (clone 2D1), and anti-CD138 PE (clone DL-101, all BD BioSciences), or doubly stained with anti-CD38 PE (BD BioSciences), then permeabilized (Fix & Perm, CALTAG Laboratories, manufacturer's directions) and stained with polyclonal goat anti-hIgG FITC (CALTAG Laboratories). Finally, the cells were fixed in 4% formaldehyde and analyzed on FC500 flow cytometer with Cytomics CXP software (Beckman Coulter, Fullerton, CA).

Drug treatment

Bortezomib (Millennium Pharmaceuticals, Inc., Cambridge, MA). This drug, formerly known as PS-341, was mixed with mannitol (in a ratio of 1:10 to increase solubility) and solubilized in 0.9% sodium chloride at the appropriate concentration before each injection. Ten days post-implantation, i.m. LAGλ-1 mice began receiving bortezomib twice weekly via i.v. tail vein injection at 0.05 or 0.5 mg/kg until the termination of the study.

Melphalan (Sigma, St. Louis, MO). The drug was solubilized in 1N hydrochloric acid, diluted to 5 mg/ml with sterile distilled water and the pH neutralized with NaOH. Appropriate concentrations were made using sterile distilled water prior to injection at 0.06, 0.6, 6.0, or 12 .0 mg/kg, starting 22 days post-implantation. Mice implanted i.m. with LAGλ-1 received intraperitoneal (i.p.) injections of melphalan once weekly.

Liposomal doxorubicin (Ortho Biotech, Bridgewater, NJ). This agent was mixed at the appropriate concentrations with sterile water prior to each injection at 0.3, 1.0, 3.0, or 10.0 mg/kg. In the first experiment, 20 days following LAGλ-1 i.m. implantation mice received i.p. liposomal doxorubicin injections once weekly. In the second experiment, 17 days post-implantation mice received i.p. liposomal doxorubicin injections once daily for three consecutive days on a weekly basis for the duration of the study.

Statistical analysis. Tumor growth and human IgG secretion curves were analyzed in terms of treatment group means and standard error. Statistical significance of differences observed in drug-treated mice versus control mice was determined using a Student's t-test. The minimal level of significance was $P<0.05$.

Results

Generating human myeloma tumors in SCID mice from MM patient BM biopsies. Fresh whole BM core biopsies from 33 individual MM patients were surgically implanted into the left hind limb superficial gluteal muscle of irradiated SCID mice. Of the 33 individual patient samples, 26 were from patients secreting IgG monoclonal proteins and seven were from patients secreting IgA. Twenty-two of the 26 mice (85%) implanted with IgG-expressing BM biopsies showed detectable human paraprotein in the serum three to four weeks post-implantation. Three of these implanted IgG biopsies produced a palpable tumor 9 to 11 weeks post-implantation. Six out of the seven mice implanted with IgA biopsies showed an increase in paraprotein levels, but none produced a palpable tumor.

Of these IgG-secreting tumors, LAGλ-1 was established through serial i.m. passages. The 74-year-old female from whom the LAGλ-1 tumor was derived presented initially with Durie-Salmon Stage IIIA IgGλ MM, and had a serum IgG level of 7470 mg/dl with multiple new lytic lesions. This patient received prior treatment with the combination of melphalan and

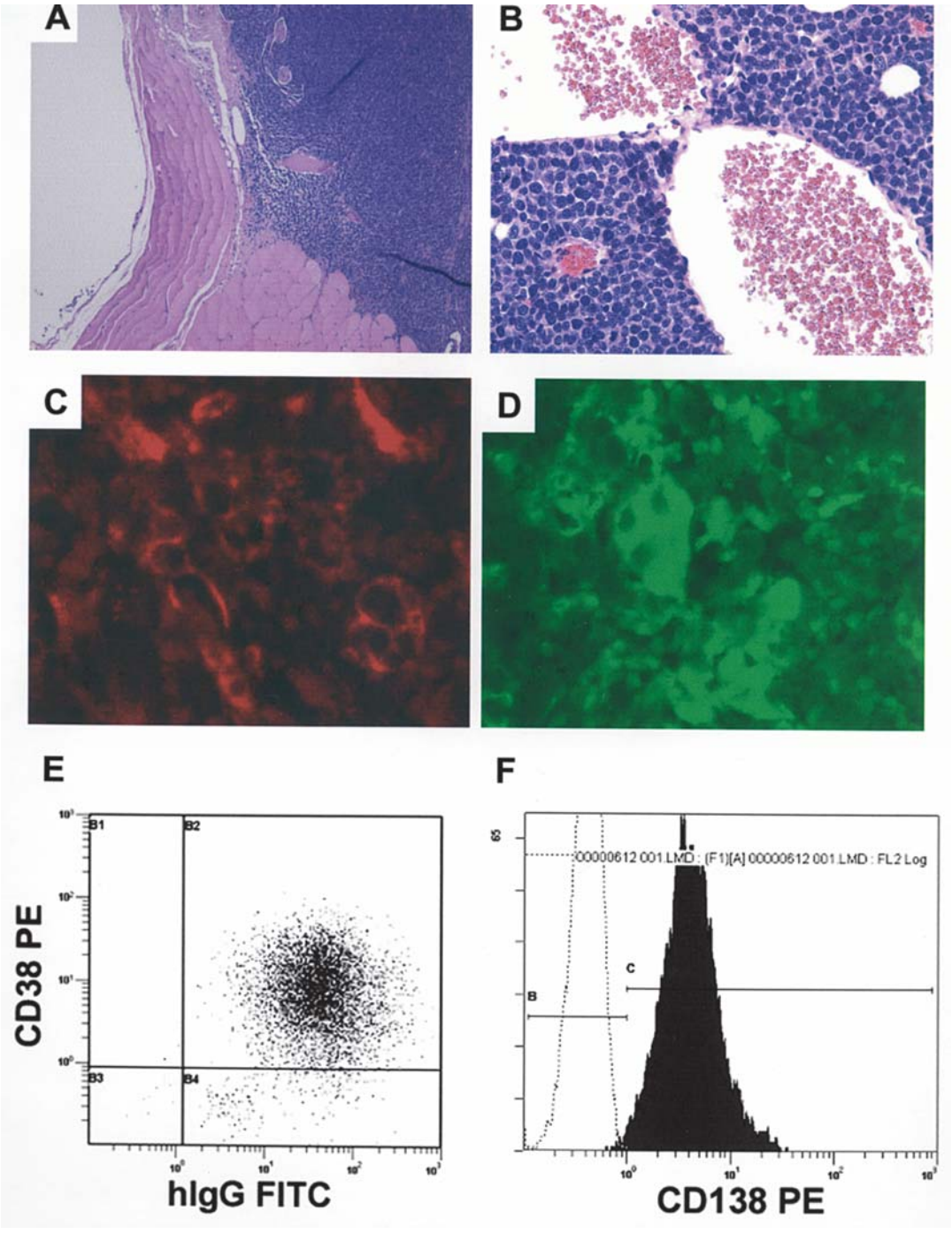

Figure 2. The LAGλ-1 tumor displays morphological and immunological features similar to human myeloma cells. (A and B) H&E staining of first generation LAGλ-1 i.m. tumor grown from a MM patient's BM biopsy reveals spherical cells with blue cytoplasm and enlarged eccentric nuclei. (C) IFA staining of tumor with CD38 demonstrates LAGλ-1 plasma cells express surface CD38. (D) The same LAGλ-1 tumor stained with anti-hIgG FITC antibody shows plasma cells with cytoplasmic hIgG. (E) Flow cytometry of a double-stained late passage single-cell suspension detects cells strongly expressing surface CD38 and cytoplasmic hIgG (96%). (F) Flow cytometric staining of tumor cells shows that LAGλ cells express the surface MM marker CD138.

prednisone, the single agent thalidomide and local radiation therapy. She did not respond to treatment with melphalan and prednisone.

Thirty days following implantation of the patient's whole core biopsy into the SCID mice, human paraprotein was detectable in the murine serum. At the time of sacrifice, hIgG levels were as high as 1700 mg/dl (Fig. 1A). A palpable tumor developed at 11 weeks post-implantation (Fig. 1A). Tumor volume was measured weekly using calipers. Twelve weeks post-implantation, the tumor measured 1.9 cm^3 and the mouse was sacrificed. To determine the clonality of the LAGλ-1 tumor, hIgG and hIgλ in the murine serum were analyzed by immunofixation electrophoresis (IFE). Monoclonal hIgG heavy and hIgλ light chains identical to the patient's paraprotein were detected (Fig. 1B). Thus, LAGλ-1 expressed the same Ig type as the myeloma patient from whom it was derived.

Biological characteristics of LAGλ-1 passage tumors. At 85 days post-implantation, the 1.9 cm^3 first generation LAGλ-1 tumor was excised from the mouse and divided into two

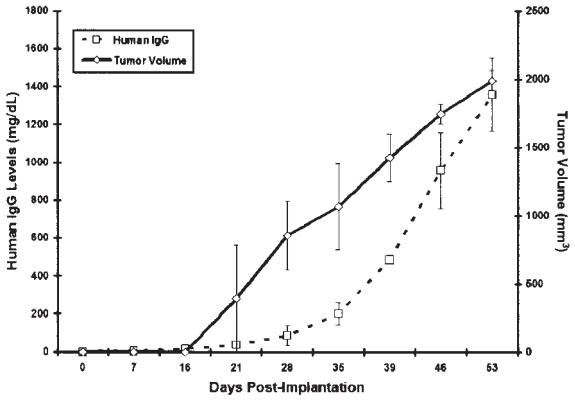

Figure 3. Fourth generation passage of LAGλ-1 displays shortened latency period of tumor growth and serum hIgG levels in SCID mice. Mouse tumors were measured weekly using standard calipers with the mean value plotted; hIgG was measured weekly by ELISA.

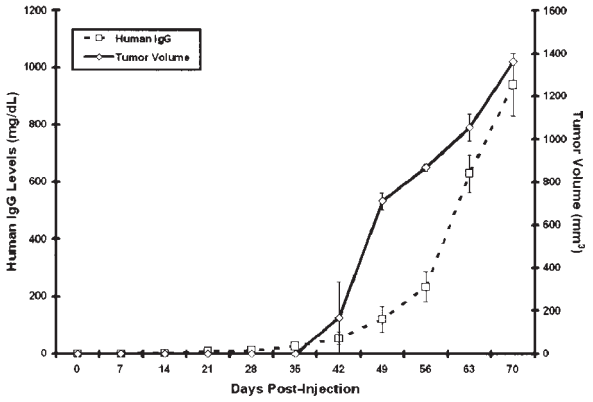

Figure 4. LAGλ-1 cells grow localized tumors when injected subcutaneously. LAGλ-1 i.m. tumor was excised and prepared as a single cell suspension and SCID mice were injected s.c. with $3x10^6$ LAGλ-1 cells. Measurable tumor growth and serum hIgG appeared ~8 weeks post injection. Tumors growing in LAGλ-1 mice were measured weekly using standard calipers and hIgG was measured weekly by ELISA.

fragments. One fragment was used to passage the tumor *in vivo* and the remainder was fixed in 10% buffered formalin and embedded in paraffin for histological analysis. Sections (4-5 μm) were cut and stained for cellular morphology with H&E. LAGλ-1 cells were rounded, contained abundant cytoplasm and displayed the typical eccentrically located nucleus found in plasma cells (Fig. 2A and B). Immunofluorescent studies showed that the cells expressed the memory/plasma B cell surface marker CD38 (Fig. 2C) and cytoplasmic hIgG (Fig. 2D). The LAGλ-1 tumors were EBV and CMV negative by IHC staining (data not shown). To confirm the stability of the LAGλ-1 model, cells from a late-passage tumor were analyzed using flow cytometry (Fig. 2E and F). A 15th generation LAGλ-1 i.m. tumor was excised and made into a single cell suspension. The cells were surface stained for CD19, CD20, CD38, CD45, CD138, and permeabilized and stained intracellularly for cytoplasmic hIgG. The LAGλ-1 tumor maintained expression of surface CD38, CD138, and cytoplasmic hIgG (Fig. 2E and F) whereas the cells did not express CD19, CD20, or CD45 (data not shown).

Although LAGλ-1 cells undergo apoptosis when cultured *in vitro* for longer than 72 h (data not shown), a series of surgical implantations allowed maintenance of the LAGλ-1 tumor *in vivo*, suggesting that LAGλ-1 requires support by the murine microenvironment.

Once the volume of the primary patient implant tumor measured 1.9 cm^3, the tumor was removed, sectioned and implanted as before. Currently, we have maintained the LAGλ-1 line for >20 consecutive i.m. passages over a period of two years. The animals implanted (~90%) with a fourth generation LAGλ-1 tumor fragment developed a measurable tumor at a mean time of four weeks post-implantation (Fig. 3). With subsequent passages, the latency period for detection of a palpable tumor markedly decreased from 11 weeks to four weeks by the fourth generation while the time to detect hIgG decreased from four weeks to three weeks (Figs. 1A and 3) suggesting that we may have selected for an aggressive proliferative population. We are currently characterizing this proliferative component.

LAGλ-1 cells grow in vivo when injected subcutaneously or intravenously. Most pre-clinical MM *in vivo* studies have evaluated drug efficacy by their effects on local s.c. tumor growth (18,19); thus, we tested whether the LAGλ-1 tumor could be maintained when it was similarly injected. We also determined whether Matrigel, a basement membrane matrix with a combination of growth factors that has been shown to favor angiogenesis (20), would have a stimulatory effect on LAGλ-1 growth. Using an established i.m. passage tumor, we generated a single cell suspension and inoculated five SCID mice s.c. in the right flank with $3x10^6$ cells and five SCID mice with the same number of cells suspended in 50% Matrigel. Paraprotein levels were first detectable in both groups at ~14 days post-inoculation (Fig. 4). There was no significant difference in the growth of the tumor between the mice given cells with or without Matrigel (data not shown).

To extend the model to include BM infiltration by LAGλ-1, we initiated tumor growth through i.v. injection of LAGλ-1 tumor cells. Using an established fifth generation LAGλ-1 i.m. tumor, we created a single cell suspension and injected $5x10^6$ LAGλ-1 cells into the tail vein of each SCID mouse. The mice showed detectable hIgG levels within 10-11 weeks (Fig. 5A), nearly 5 times longer than the time required for the appearance of hIgG in the serum of i.m. LAGλ-1 tumor-bearing SCID mice. At the time of euthanasia, ~50% of these mice showed signs of hind limb paralysis, evidence of myeloma cell infiltration into the marrow space and bone resorption. Most notably, the LAGλ-1 myeloma cells metastasized and heavily infiltrated the murine tibia (Fig. 5D). Moreover, histological analysis of tissues harvested at the time of sacrifice confirmed MM cell infiltration into the murine liver (Fig. 5B) and spleen (Fig. 5C). Other tissues with myeloma cell infiltration also included the murine lung and kidneys (data not shown).

Growth of LAGλ-1 is markedly inhibited by bortezomib and liposomal doxorubicin but only minimally by melphalan. In order to test the clinical relevance of our MM mouse model and show that the LAGλ-1 tumor could produce large numbers of animals for efficient testing of drugs in pre-clinical studies, we studied the activity of bortezomib, a proteasome inhibitor with known anti-myeloma effects (21), in i.m. LAGλ-1-

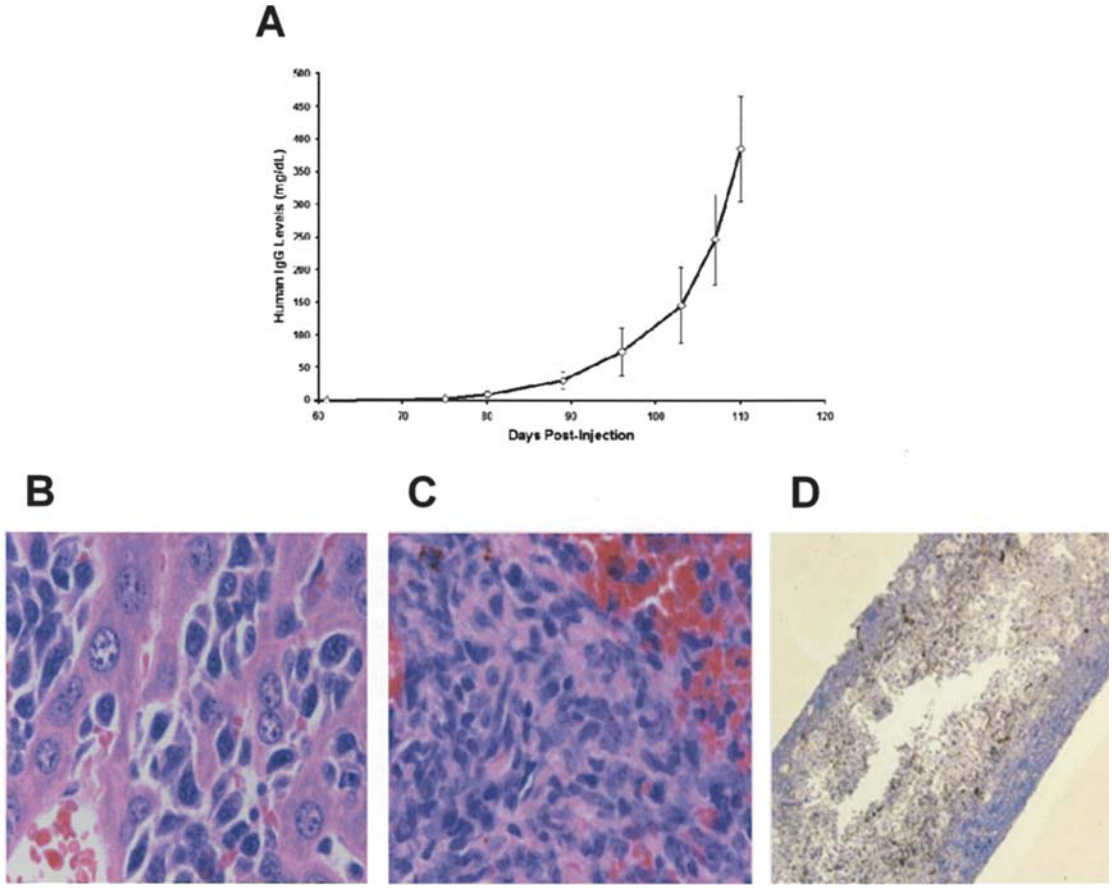

Figure 5. LAGλ-1 cells grow systemic tumors when injected intravenously. LAGλ-1 i.m. tumor was excised and made into a single cell suspension. Tumor cells ($5x10^6$) were injected i.v. into the tail vein of 10 SCID mice. (A) Serum hIgG levels in SCID mice following i.v. injection increases ~16 weeks after LAGλ-1 inoculation. (B) H&E staining of murine liver demonstrates LAGλ-1 cell infiltration. (C) H&E staining of murine spleen demonstrates LAGλ-1 cell infiltration. (D) IHC staining of murine tibia shows hIgG positive LAGλ-1 cells have infiltrated into the SCID BM.

bearing mice. Twelve irradiated SCID mice implanted with 2-6 mm^3 LAGλ-1 tumor fragments developed measurable tumors and detectable levels of serum hIgG. Once the tumor was palpable at 17 days post-implantation, mice were blindly assigned to 1 of 3 treatment groups, including: 0.05 mg/kg bortezomib (n=4), 0.5 mg/kg bortezomib (n=4), or 0.9% normal saline control (n=4). The drug or saline was administered i.v. twice weekly. Animals treated with the lower dose of bortezomib (0.05 mg/kg) showed similar paraprotein secretion (Fig. 6A) and tumor growth characteristics (Fig. 6B) to those animals receiving control saline. In contrast, those animals receiving the higher dose (0.5 mg/kg) of the proteasome inhibitor showed significant inhibition of LAGλ-1, compared to control animals, as demonstrated by both reduced tumor growth (P=0.004) and decreased hIgG secretion (P=0.003; Fig. 6A and B).

We wished to further validate our LAGλ-1 model by determining whether the tumor maintained in the SCID mice continued to show the melphalan resistance of the original patient's disease. Mice (n=23) were implanted with a 2-6 mm^3 LAGλ-1 tumor fragment i.m. Once the tumor was detectable, the animals were randomized into four separate melphalan treatment groups (0.06, 0.6, 6.0, or 12.0 mg/kg, n=5 each), or a 0.9% normal saline control group (n=3). Melphalan was administered i.p. once weekly, starting 22 days post-implantation. Animals treated with melphalan at doses ≤6.0 mg/kg showed similar tumor growth to those receiving vehicle alone (Fig. 6C). Only animals receiving the highest dose (12.0 mg/kg) showed a minimal decrease in tumor growth compared to those treated with vehicle alone (P<0.04, Fig. 6C). This dose was 20 times higher than the dose that produced significant growth inhibition of the melphalan-sensitive MM cell line RPMI-8226, when similarly implanted in SCID mice (Fig. 6D). SCID mice bearing s.c. RPMI-8226 tumors were treated with various doses of melphalan (0.006, 0.06, and 0.6 mg/kg, n=3/group) once weekly via i.p. injection. A dose of 0.6 mg/kg was sufficient to significantly slow tumor growth compared to other doses and vehicle alone. Therefore, the LAGλ-1 i.m. model exhibits melphalan resistance similar to that of the original MM patient's disease.

Finally, we investigated the anti-myeloma effects of liposomal doxorubicin and optimized the drug's dosing schedule using the LAGλ-1 i.m. model. Twenty days post-implantation, mice bearing i.m. LAGλ-1 received weekly i.p. injections of liposomal doxorubicin at 0.3, 1.0, 3.0, or 10 mg/kg, or 0.9% saline (four mice in each treatment group). No anti-myeloma effects were seen at even the highest dose (data not shown). When we administered this drug more frequently, however, marked anti-tumor effects were observed with low doses of liposomal doxorubicin. When the tumor was detectable (17 days post-implantation) mice were blindly assigned to 1 of 4 treatment groups, liposomal doxorubicin at 0.3, 1.0, or 3.0 mg/kg, or a saline control group (four mice in each treatment group). Liposomal doxorubicin or saline were administered i.p.

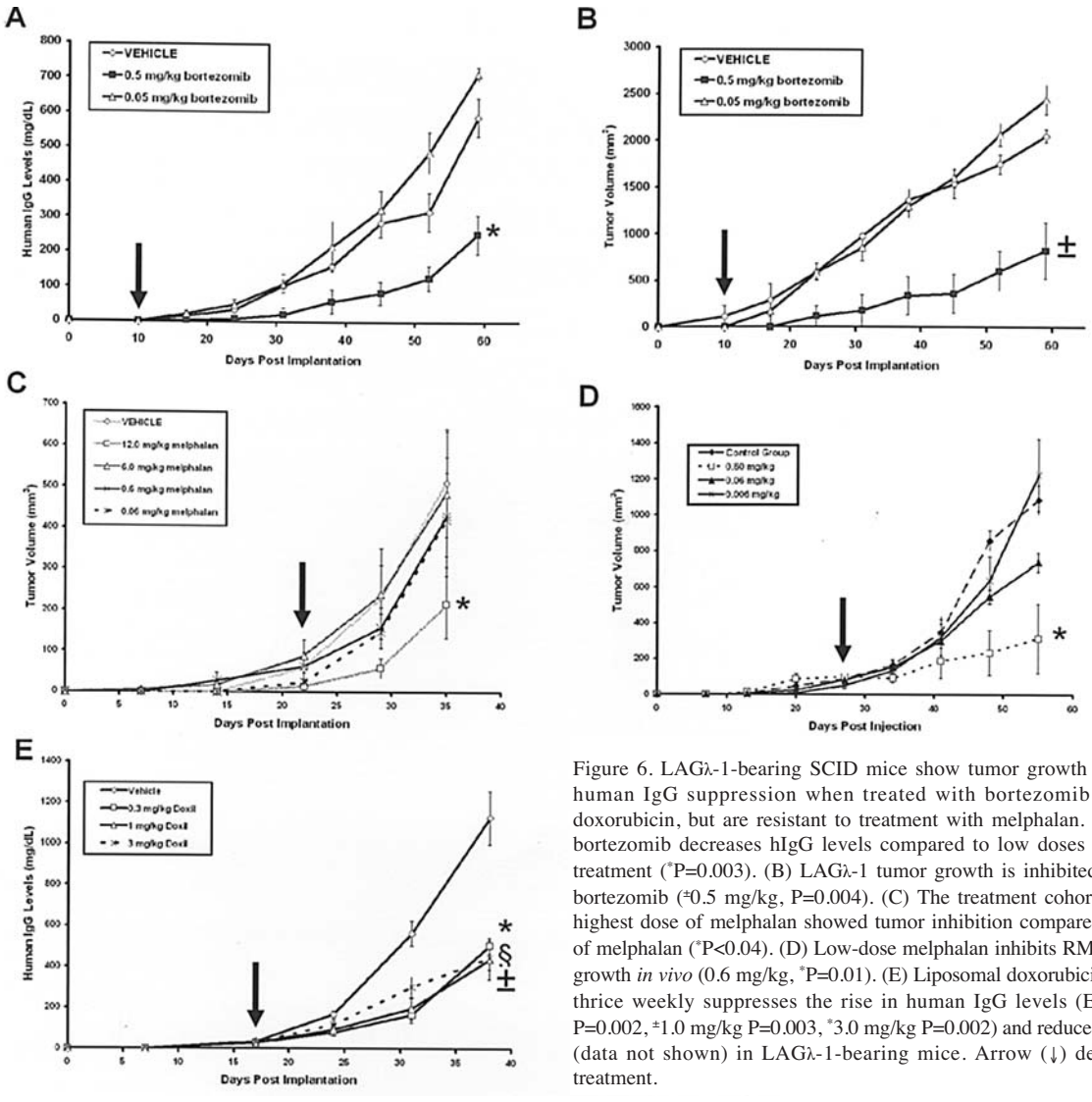

Figure 6. LAGλ-1-bearing SCID mice show tumor growth inhibition and human IgG suppression when treated with bortezomib or liposomal doxorubicin, but are resistant to treatment with melphalan. (A) High-dose bortezomib decreases hIgG levels compared to low doses of bortezomib treatment (*P=0.003). (B) LAGλ-1 tumor growth is inhibited by high-dose bortezomib (±0.5 mg/kg, P=0.004). (C) The treatment cohort receiving the highest dose of melphalan showed tumor inhibition compared to low doses of melphalan (*P<0.04). (D) Low-dose melphalan inhibits RMPI-8226 tumor growth *in vivo* (0.6 mg/kg, *P=0.01). (E) Liposomal doxorubicin administered thrice weekly suppresses the rise in human IgG levels (E) ($0.3 mg/kg P=0.002, ±1.0 mg/kg P=0.003, *3.0 mg/kg P=0.002) and reduces tumor growth (data not shown) in LAGλ-1-bearing mice. Arrow (↓) denotes start of treatment.

once daily for three consecutive days weekly for the duration of the study. Marked inhibition of LAGλ-1 was found in all three groups of SCID mice that received liposomal doxorubicin with this more frequent dosing schedule. Tumor inhibition was observed even among animals that received the lowest dose thrice weekly (0.3 mg/kg/dose = 0.9 mg/kg/week) which was <10% of the weekly dose (10 mg/kg) that had no anti-myeloma effect when administered once weekly. Specifically, animals treated with thrice weekly liposomal doxorubicin showed decreased hIgG serum levels (0.3 mg/kg, P=0.002; 1.0 mg/kg, P=0.003; 3.0 mg/kg, P=0.002; Fig. 6E). Moreover, a similar reduction in tumor size was also observed in the groups that received this more frequent treatment schedule (data not shown). These results show that marked differences in the anti-myeloma effects of this anthracycline can be achieved with a simple adjustment of the dosing schedule, and suggest that a more frequent administration of lower doses of this drug may improve its efficacy for myeloma patients while also reducing its side effects.

Discussion

The present study demonstrates that the newly developed drug resistant MM tumor model, LAGλ-1, bears similar characteristics to human MM and allows effective and rapid evaluation of new anti-myeloma treatments. Further, this MM model will improve our understanding of the biology of myeloma and drug resistance. Tumor growth was initially generated from the i.m. implantation of fresh BM biopsies from MM patients. While only three SCID mice implanted with MM BM biopsies generated palpable tumors, 85% (28/33) of the mice had evidence of tumor growth as indicated by the presence of detectable serum hIgG paraprotein levels. Subsequently, extramedullary tumors that grew from the BM implants were excised and passaged into recipient mice to preserve the malignant clone and establish large numbers of tumor-bearing mice with short latency periods before appearance of detectable tumor. Even after 25 passages, the LAGλ-1 tumor retains the morphologic and immunologic features of the patient's original myeloma cells, including the expression of CD38, CD138, hIgG, and hIgλ light chains. Furthermore, mice implanted with LAGλ-1 tumor exhibit characteristics of the MM patient's disease from whom the BM biopsy was taken, including plasma cell infiltration and increasing serum human IgG paraprotein levels. During the first several passages, the latency period for both human IgG detection and palpable tumor decreased significantly, suggesting that we may have selected for the proliferative

component of this myeloma tumor. LAGλ-1-bearing mice developed from passage of *in vivo* tumors produce elevated serum hIgG within 10 days and palpable tumors within 20 days of implantation. Notably, the cells undergo apoptosis within 72 h when the LAGλ-1 tumor is prepared as a single cell suspension, and cultured *ex vivo* in RPMI-1640 supplemented with 10% FBS. Thus, LAGλ-1 cannot sustain growth without a supportive *in vivo* environment distinguishing itself from the traditional cell lines that are often used to generate MM tumors in immunodeficient mice.

The LAGλ-1 model provides multiple advantages over currently available animal models for the evaluation of new treatment strategies for MM. First, the s.c. and i.v. routes of administration of LAGλ-1 cells allow quantification of the number of cells injected. Thus, a known number of cells can be injected in mice and produce very similar growth patterns as determined by measuring hIgG levels and tumor volume curves. Second, the i.m. and s.c. models provide tumors that are detectable early and measured precisely, and a large cohort of SCID mice with tumors that grow rapidly in a consistent and reproducible fashion. Third, the short latency period and subsequent rapid growth of these tumors establish an efficient model to quickly determine the potential efficacy of drugs within two weeks of the initiation of treatment. Finally, LAGλ-1 retains the original chemoresistant phenotype displayed by the donor myeloma patient. Experiments investigating the mechanisms behind drug resistance and low dose combination studies to chemosensitize LAGλ-1 will help shape the future of treating relapsed and refractory myeloma patients.

Previous animal studies have shown numerous advantages in using tumors implanted s.c. for evaluating novel treatments for MM (2,10,18,19). To adapt our model for use in the preclinical evaluation of new anti-MM therapies, we also expanded the LAGλ-1 model to include s.c as well as i.v.-administered tumor cells. Single cell suspensions of LAGλ-1 tumors with known concentrations of cells injected s.c. or i.v., resulted in tumor proliferation and secretion of hIgG paraprotein. By growing LAGλ-1 tumors s.c., we were able to precisely measure tumor growth at the site of localization. Furthermore, SCID mice injected i.v. with LAGλ-1 develop hind-limb paralysis and post-sacrificial histology demonstrated that these tumor cells homed to the murine bone. The LAGλ-1 cells also migrated to other organs in the SCID mice when injected i.v., including the liver, lungs, kidneys, and spleen. This may be due to the large number of cells that were injected in these animals. We are currently investigating the effects of smaller numbers of LAGλ-1 cells injected i.v. which may allow for *in vivo* growth within only the BM compartment.

In order to further test the clinical relevance of LAGλ-1, studies were conducted with bortezomib, melphalan and liposomal doxorubicin using the rapidly growing i.m. model. Clinically, these drugs have been shown to have substantial anti-MM effects (22-24,26). Our studies showed that melphalan-resistant LAGλ-1 was sensitive to the anti-MM effects of bortezomib. Higher doses of bortezomib (0.5 mg/kg) reduced tumor volume and serum paraprotein levels in the LAGλ-1-bearing mice nearly three-fold whereas the lower dose (0.05 mg/kg) had no effect on tumor volume and serum paraprotein levels. These results are consistent with other studies evaluating the anti-myeloma effects of this proteasome inhibitor in the *in vivo* pre-clinical setting (18,25).

Liposomal doxorubicin has recently shown efficacy in the treatment of MM (26). We injected liposomal doxorubicin at 1.0, 3.0, and 10.0 mg/kg once weekly to LAGλ-1-bearing SCID mice. Using this dosing schedule, the LAGλ-1 tumor model did not respond to this anthracycline even at the highest dose. In contrast, when the drug was administered more frequently (thrice weekly), marked inhibition of LAGλ-1 was found even among animals that received the lowest dose (0.3 mg/kg/dose). These data suggest that in addition to dosage, scheduling optimization can also be critical to evaluating drug efficacy and may allow administration of lower but equally effective doses. Using the LAGλ-1 model, we can quickly and efficiently evaluate drug dosing and optimize schedules, an aspect of drug development that has not been adequately addressed with many agents.

In addition to facilitating drug development, the LAGλ-1 model can also be used to study the biology of drug resistance in MM. Since the original LAGλ-1 BM biopsy was obtained from a patient resistant to melphalan-based therapy, we also tested the melphalan resistance of the tumor in the SCID mice. LAGλ-1 tumors proved to be resistant to this alkylating agent with only minimal anti-tumor effects observed among animals that received the highest dose of the drug. This dose (12.0 mg/kg) was much higher than doses of melphalan that produced anti-myeloma effects in SCID mice bearing the RPMI-8226 cell line as well as mice growing other MM cell lines (27-29). Hence, the LAGλ-1 tumors retained the melphalan resistance of the MM patient's cancer cells showing that although this human myeloma has been maintained through serial passages in SCID mice, the characteristics of the patient's original tumor's drug resistance were unaltered. We are currently investigating the mechanism(s) of LAGλ-1's resistance to melphalan which may help to determine ways to overcome melphalan resistance in MM patients. Preliminary data using this same intramuscularly implanted LAGλ-1 tumor model suggest that doses of arsenic trioxide, a drug that reduces nuclear factor kappa B (NF-κB) activity, that have no anti-MM effects alone against LAGλ-1, can be combined with low doses of melphalan to effectively treat this tumor in SCID mice (data not shown). These results suggest that strategies can be developed using this tumor model to help overcome chemoresistance for patients with multiple myeloma (30,31).

The LAGλ-1 model described here should help hasten the development of new agents as well as optimizing dose, schedule and ultimately more effective combination therapies for MM patients. The LAGλ-1 murine model also provides us with the ability to select the most suitable method of investigation for each specific pre-clinical drug study. For example, s.c. tumor growth can be used to analyze anti-proliferative effects whereas growth in the BM following i.v. injection of cells can be used to determine inhibition of bone resorption by anti-MM drugs and effects of novel anti-bone resorptive agents. Studies are currently underway to generate cells that specifically home to the bone marrow microenvironment. In addition, these different models should allow the separation of anti-tumor effects outside of the bone to bone-related anti-MM activity.

The LAGλ-1 SCID mouse model provides an opportunity to further characterize the pathophysiology of human MM and to rapidly assess and optimize the development of new therapies and targets to more effectively treat and expand the treatment options for patients with multiple myeloma.

The success of the LAGλ-1 model is not unique to this particular tumor. Other tumors derived from other patients have been established and passaged *in vivo*. These will be analyzed subsequently. Furthermore, it is possible that with methods to improve the efficacy of take to close to 100% we should be able to determine treatment strategies with individual tumors to treat respective patients.

Acknowledgements

We wish to acknowledge Regina Swift for helpful discussions, S. Gibb Jarutirasarn and Christine Pan James for assistance with the preparation of this report. This study was supported by the Myeloma Research Fund and the Annenberg, Kramer and Skirball Foundations.

References

1. Alsina M, Boyce BF, Devlin RD, *et al*: Development of an *in vivo* model of human multiple myeloma bone disease. Blood 87: 1495-1501, 1996.
2. Bellamy WT, Mendibles P, Bontje P, *et al*: Development of an orthotopic SCID mouse-human tumor xenograft model displaying the multidrug-resistant phenotype. Cancer Chemother Pharmacol 37: 305-316, 1996.
3. Dewan MZ, Watanabe M, Terashima K, *et al*: Prompt tumor formation and maintenance of constitutive NF-κB activity of multiple myeloma cells in NOD/SCID/γc^{null} mice. Cancer Sci 95: 564-568. 2004.
4. Mitsiades CS, Mitsiades NS, Bronson RT, *et al*: Fluorescence imaging of multiple myeloma cells in a clinically relevant SCID/NOD *in vivo* model: biologic and clinical implications. Cancer Res 63: 6689-6696, 2003.
5. Miyakawa Y, Ohnishi Y, Tomisawa M, *et al*: Establishment of a new model of human multiple myeloma using NOD/SCID/γc^{null} (NOG) mice. Biochem Biophys Res Commun 313: 258-262, 2004.
6. Reme T, Gueydon E, Jacquet C, *et al*: Growth and immortalization of human myeloma cells in immunodeficient severe combined immunodeficiency mice: a preclinical model. Br J Haematol 114: 406-413, 2001.
7. Urashima M, Chen BP, Chen S, *et al*: The development of a model for the homing of multiple myeloma cells to human bone marrow. Blood 90: 754-765, 1997.
8. Ashmann EMJ, van Tol MDJ, Oudemann-Gruber J, *et al*: The SCID mouse as a model for multiple myeloma. Br J Haematol 89: 319-327, 1995.
9. Feo-Zuppardi J, Taylor CW and Iwato K: Long-term engraftment of fresh human myeloma cells in SCID mice. Blood 80: 2843-2850, 1992.
10. Huang SY, Tien HF, Su FH and Hsu SM: Nonirradiated NOD/SCID-human chimeric animal model for primary human multiple myeloma. Am J Pathol 164: 747-756, 2004.
11. Kyoizumi S, Baum CM, Kaneshima H, McCune JM, Yee EJ and Namikawa R: Implantation and maintenance of functional human bone marrow in SCID-hu mice. Blood 79: 1704-1711, 1992.
12. Namikawa R, Ueda R and Kyoizumi S: Growth of human myeloid leukemias in the human marrow environment of SCID-hu mice. Blood 82: 2526-2536, 1993.
13. Pilarski LM, Hipperson G, Seeberger K, *et al*: Myeloma progenitors in the blood of patients with aggressive or minimal disease: engraftment and self-renewal of primary human myeloma in the bone marrow of NOD/SCID mice. Blood 95: 1056-1065, 2000.
14. Radl J: Multiple myeloma and related disorders. Lessons from an animal model. Pathol Biol (Paris) 47: 109-114, 1999.
15. Yaccoby S and Epstein J: The proliferative potential of myeloma plasma cells manifest in the SCID-hu host. Blood 94: 3576-3582, 1999.
16. Yaccoby S, Barlogi B and Epstein J: Primary myeloma cells growing in SCID-hu mice: a model for studying the biology and treatment of myeloma and its manifestations. Blood 92: 2908-2913, 1998.
17. Yata K and Yaccoby S: The SCID-rab model: a novel *in vivo* system for primary human myeloma demonstrating growth of CD138-expressing malignant cells. Leukemia 18: 1891-1897, 2004.
18. LeBlanc R, Catley LP, Hideshima T, *et al*: Proteasome inhibitor PS-341 inhibits human myeloma cell growth *in vivo* and prolongs survival in a murine model. Cancer Res 62: 4996-5000, 2002.
19. Frost P, Moatomed F, Hoang B, *et al*: *In vivo* anti-tumor effects of the mTOR inhibitor, CCI-779, against human multiple myeloma cells in a xenograft model. Blood 104: 4181-4187, 2004.
20. Lentzsch S, Rogers MS, LeBlanc R, *et al*: S-3-Amino-phthalimido-glutarimide inhibits angiogenesis and growth of B-cell neoplasias in mice. Cancer Res 62: 2300-2305, 2002.
21. Richardson PG, Barlogie B, Berenson J, *et al*: A phase 2 study of bortezomib in relapsed, refractory myeloma. N Engl J Med 348: 2609-2617, 2003.
22. Dimopoulos MA and Kyle RA: Treatment of multiple myeloma. In: Biology and Management of Multiple Myeloma. Berenson JR (ed). Humana Press, New Jersey, pp137-151, 2004.
23. Sirohi B and Powles R: Multiple myeloma. Lancet 363: 875-887, 2004.
24. Berenson JR, Yang HH, Sadler K, *et al*: Phase I/II trial assessing bortezomib and melphalan combination therapy for the treatment of patients with relapsed or refractory multiple myeloma. J Clin Oncol 24: 937-944, 2006.
25. Hussein MA, Wood L, His E, *et al*: A phase II trial of pegylated liposomal doxorubicin, vincristine, and reduced-dose dexamethasone combination therapy in newly diagnosed multiple myeloma patients. Cancer 95: 2160-2168, 2002.
26. Orlowski RZ, Voorhees PM, Garcia RA, *et al*: Phase 1 trial of the proteasome inhibitor bortezomib and pegylated liposomal doxorubicin in patients with advanced hematologic malignancies. Blood 105: 3058-3065, 2005.
27. Basu S, Ma R, Boyle PJ, *et al*: Apoptosis of human carcinoma cells in the presence of potential anti-cancer drugs: III. Treatment of Colo-205 and SKBR3 cells with: cis-platin, tamoxifen, melphalan, betulinic acid, L-PDMP, L-PPMP, and GD3 ganglioside. Glycoconj J 20: 563-577, 2004.
28. Furrer M, Altermatt HJ, Ris HB, *et al*: Lack of antitumour activity of human recombinant tumour necrosis factor-alpha, alone or in combination with melphalan in a nude mouse human melanoma xenograft system. Melanoma Res 7: S43-S49, 1997.
29. Uneda S, Hata H, Matsuno F, *et al*: A nitric oxide synthase inhibitor, N(G)-nitro-l-arginine-methyl-ester, exerts potent anti-angiogenic effects on plasmacytoma in a newly established multiple myeloma severe combined immunodeficient mouse model. Br J Haematol 120: 396-404, 2003.
30. Berenson JR, Ma HM and Vescio R: The role of nuclear factor-kappaB in the biology and treatment of multiple myeloma. Semin Oncol 28: 626-633, 2001.
31. Ma MH, Yang HH, Parker K, *et al*: The proteasome inhibitor PS-341 markedly enhances sensitivity of multiple myeloma tumor cells to chemotherapeutic agents. Clin Cancer Res 9: 1136-1144, 2003.